  DOI 10.1515/htmp-2012-0032

Dissolution Behavior of Dicalcium Silicate and Tricalcium Phosphate Solid Solution and other Phases of Steelmaking Slag in an Aqueous Solution

Takuya Teratoko,[1] Nobuhiro Maruoka,[2,*] Hiroyuki Shibata[2] and Shin-ya Kitamura[2]

[1] Hitachi Metals Ltd., Yasugi, Shimane, Japan

[2] Institute of Multidisciplinary Research for Advanced Materials, Tohoku University, Aoba ku, Sendai, Japan

Abstract. Most of the phosphorus in slag forms a solid solution of dicalcium silicate (C_2S) and tricalcium phosphate (C_3P), and the process used to separate this solid solution from the matrix phase is the same technology used to separate P from other valuable elements such as Mn and Cr containing in the matrix phase. Although it is known that the solubility of C_2S in an aqueous solution is much greater than that of C_3P, the solubility of the solid solution and that of the matrix phase have yet to be investigated. To clarify the possibility of selectively extracting P from slag through a leaching process, the dissolution behaviors of the solid solution at various compositions and that of the matrix phase were investigated. The following results were obtained: The dissolution ratio of Ca to the aqueous solution at pH = 7 was close to 1.0 in the case of pure C_2S and decreased greatly with increasing C_3P content. The dissolution ratio of P was about 0.1 and did not change relative to the C_3P content. When the ratio of C_3P in the solid solution was higher than 0.3, hydroxyapatite (HAP) formation was observed in the residue. The dissolution ratio of P increased for 30 min, and after reaching the maximum value, started to decrease owing to the precipitation of HAP. The dissolution ratio of each element from a glassy slag sample (matrix phase) was lower than that from the solid solution at every pH level.
In this study, the possibility to extract a solid solution containing P without dissolving the matrix phase was found through the use of an aqueous solution at pH = 7, although the dissolution ratio of P was not sufficiently high.

Keywords. Phosphorus, steelmaking slag, extraction, leaching, pH.

PACS®(2010). 05.70.-a, 88.10.jp.

* **Corresponding author:** Nobuhiro Maruoka, Institute of Multidisciplinary Research for Advanced Materials, Tohoku University, 2-1-1 Katahira, Aoba ku, Sendai 980-8577, Japan; E-mail: maruoka@tagen.tohoku.ac.jp.

1 Introduction

It is well known in the steelmaking industry, various characteristics of steel products are controlled by the addition of alloying metals. In the recycling of steel scrap, the scrap is used for the production of low-grade steel and the value of the added alloying elements is not considered. Owing to an increase in the demand for high-purity alloying metals, the recycling of such metals in the steelmaking process is necessary.

Steelmaking slag contains many valuable elements and can be considered a domestic resource of alloying elements, especially Mn and Cr. These elements can be easily separated from slag in the form of a ferroalloy using reduction reactions; however, the ratio of Mn and Cr to Fe is too low and the P content too high for the use of this ferroalloy in the steelmaking process. Therefore, we propose an innovative process to separate P from Mn [1]. In this process, steelmaking slag is sulfurized and a FeS-MnS-CaS matte is formed. As P does not form a stable sulfide, P is not distributed to the matte phase. However, as Cr also does not form a stable sulfide, the separation of Cr is not achievable through this process.

Cr is mainly used as an alloying metal to produce stainless steel. Stainless steel is divided into two types based on the metallography: austenitic stainless steel, which contains Cr and Ni, and ferritic stainless steel, which contains Cr but no Ni. Although most steel scrap exhibits magnetic properties, austenitic stainless steel is non-magnetic. Consequently, austenitic stainless steel scrap is easily separated from other steel scrap. Unlike austenitic stainless steel scrap, ferritic stainless steel scrap is magnetic, which makes it difficult to separate from plain carbon steel scrap. This results in an increase in the Cr content in the scrap used to produce plain carbon steel, and an increase in the Cr content of EAF slag, as Cr is oxidized during the refining process. Oda et al. showed [2] that about 80% of Cr in ferritic stainless steel scrap is recovered in plain carbon steel scrap and that the Cr content in the scrap used to produce plain carbon steel is increasing.

Steelmaking slag, including hot metal dephosphorization slag, can be considered to be within the CaO-SiO_2-FeO-P_2O_5 system and is usually in the dicalcium silicate (C_2S) saturated composition range. It is well known that

Received: February 14, 2012. Accepted: March 3, 2012.

C_2S forms a pseudo-binary solid solution with tricalcium phosphate (C_3P) over a wide composition range at steelmaking temperatures. Measurements of the equilibrium distribution ratio of P_2O_5 between the solid solution and liquid phase of the slag have revealed that P_2O_5 is concentrated in the solid solution with a high distribution ratio [3]. This implies that most of the P in the slag forms the solid solution, and the process used to separate this solid solution from the matrix phase is the same technology used to separate P from other valuable elements such as Mn and Cr containing in the matrix phase. Different methods to separate the solid solution using the differences in the physical properties of both phases have been previously reported. Ono et al. tried to separate a solid solution using the differences in density [4]. The density of the solid solution is about 2.75 g/cm^3, which is lower than that of the residual liquid phase (3.14 g/cm^3). Therefore, during the slow cooling of slag, the solid solution floats on top of the residual liquid. By cutting the slag ingots after solidification, the phosphorus containing phase can be separated from the other phases. The authors have concluded that when the cooling rate is slower than 1.5 °C/min, more than 70% of the P can be separated. On the contrary, Nagasaka et al. tried to separate the solid solution using the differences in the magnetic property [5]. They revealed that the solid solution has a diamagnetic property with weak magnetization, whereas the FeO-containing matrix phase shows ferromagnetism or paramagnetism with a relatively strong magnetization. By using a superconducting magnet with a generated surface magnetic field strength of 2.5 T, a cell containing water and a grounded slag with a particle size of less than 32 μm was treated. The authors have concluded that about 62% of the solid solution can be recovered through this procedure. These methods are effective for using the matrix phase as a refining flux, and the solid solution as a phosphate resource for fertilizers. Nevertheless, to use the matrix phase as a raw material of ferro-chromium alloy, the separation rate is not sufficiently high.

On the other hand, if the dissolution rate of the solid solution in an aqueous solution is higher than that of the matrix phase, the separation of the solid solution using a leaching treatment becomes possible. The dissolution behaviors of various elements from slag in seawater have been investigated. Miki et al. [6] showed the solubility of C_2S and C_3P in seawater. Based on their results, the solubility of C_2S is much greater than that of C_3P, and the solubility of both phases decreases with an increase in pH. However, the solubility of the solid solution and that of the matrix phase in water has yet to be investigated.

Based on these backgrounds, to clarify the possibility of the selective extraction of phosphorus from slag through leaching, the dissolution behavior of the solid solution with various compositions and matrix phase were investigated.

2 Experimental Method

2.1 Preparation of Oxide Samples

For the preparation of C_2S, a mixture of reagent-grade $CaCO_3$ and SiO_2 with a target composition of CaO-34.9 mass% SiO_2 was pressed to form a disc of 13 mm in diameter, and then heated at 1773 K for 24 h. After cooling, γ-C_2S powder was obtained, since the disc disintegrated due to the volume expansion caused by the phase transformation. The formation of dicalcium silicate was confirmed using X-ray diffraction analysis. For the preparation of C_3P, reagent-grade C_3P was heated at 1873 K in an air atmosphere for 48 h and cooled in a furnace. To prepare the solid solution of C_2S and C_3P, γ-C_2S powder, made using the above method, and reagent-grade C_3P were mixed according to the appropriate ratio, pressed into a disc of 13 mm in diameter, and then heated at 1873 K for 48 h. After cooling, the phase of the solid solution was determined through X-ray diffraction analysis. The composition ratio of C_2S and C_3P in terms of mass%, and the determined phases are summarized in Table 1. The name of each phase corresponds to that in the phase diagram shown in Figure 1 [7]. Compare with the phase diagram, only those phases that are stable at lower temperature were observed, even though only the R phase is stable at 1873 K in each composition ratio. These phases are considered to be precipitated during the cooling of the samples.

For the production of CaO, reagent grade $CaCO_3$ was heated at 1273 K for 60 min or more under an air atmosphere in an Al_2O_3 crucible. To prepare the slag of a CaO-SiO_2-P_2O_5-Fe_2O_3 system, reagent grade SiO_2, Fe_2O_3, and $3CaO \cdot P_2O_5$, along with CaO produced using the above method, were mixed and heated in a Pt crucible under an air atmosphere. To prepare the slag of a CaO-SiO_2-P_2O_5-FeO system, SiO_2, Fe_2O_3, CaO, and electrolytic iron were mixed and heated in a steel crucible under an Ar-3%H_2 atmosphere. When the slag containing a large volume fraction of the solid solution was made, the mixed reagent was pressed into a disc and heated at 1613 K or 1723 K for 48 h and then quenched by water. In this paper, this type of sample is called a "solid solution with a matrix phase." The composition of the solid solution with a matrix phase is summarized in Table 2. When the slag containing a small volume fraction of the solid solution or the slag without containing solid solution was made, the mixed reagent was put into a crucible and heated. This sample type is called "synthesized steelmaking slag" in this paper. The slag composition and heating pattern are summarized in Tables 3 and 4, respectively. In the heating pattern shown in Table 4, the maximum temperature was determined to melt the slag and cooled to precipitate the solid solution from the liquid slag.

The quenched sample was mounted and polished. The composition of each phase was measured using an electron probe micro analyzer (EPMA). In addition, the precipitated phases were determined using X-ray diffraction analysis.

Sample number		*1*	*2*	*3*	*4*	*5*	*6*	*7*	*8*	*9*	*10*	*11*
C_2S:C_3P		10:0	9:1	8:2	7:3	6:4	5:5	4:6	3:7	2:8	1:9	0:10
$C_3P/(C_2S+C_3P)$		0	0.1	0.2	0.3	0.4	0.5	0.6	0.7	0.8	0.9	1.0
Phases	Before dissolution	γ-C_2S	α'-C_2S	α'-C_2S	R	R	A	A, S	S	α-C_3P, R	α-C_3P	α-C_3P
	After dissolution	amorphous SiO_2	amorphous SiO_2	amorphous SiO_2	HAP	HAP	HAP	S	S	R, HAP	HAP	α-C_3P

Table 1. Composition ratio of C_2S and C_3P in terms of mass% and the determined phase before and after the dissolution experiment.

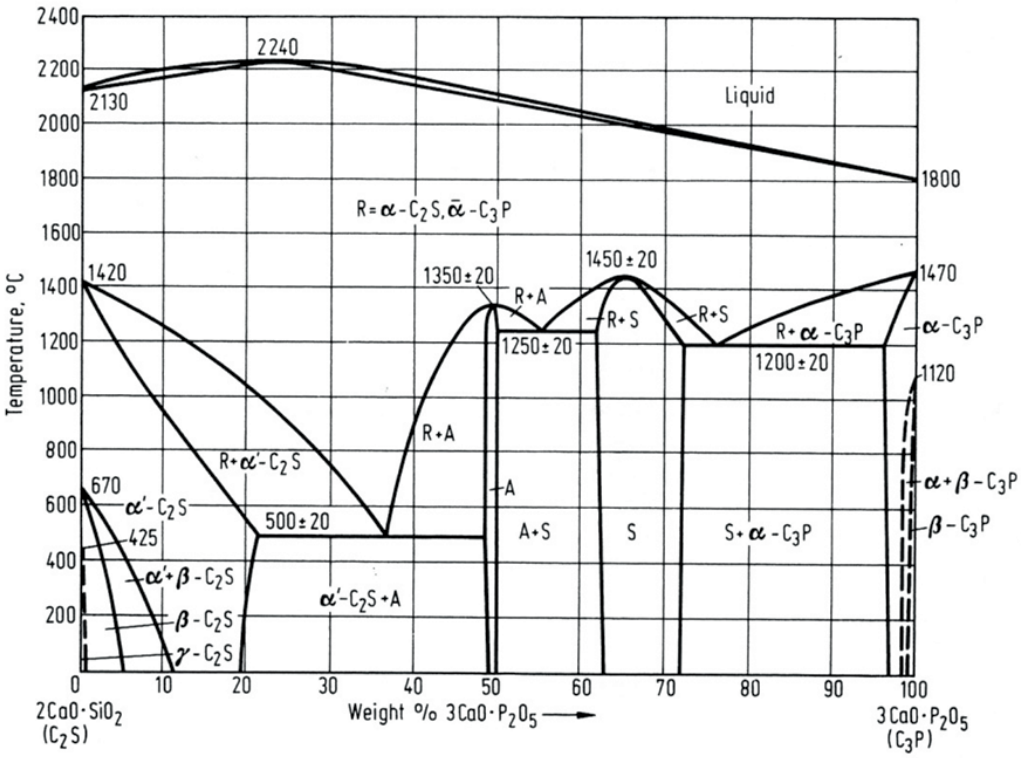

Figure 1. Phase diagram of 2CaO•SiO_2-3CaO · P_2O_5 system. [7]

name	CaO	SiO_2	P_2O_5	FeO	Fe_2O_3
SS2+	52.5	24.9	13.7	8.9	0
SS3+(1)	60.4	24.4	13.7	0	1.5
SS3+(2)	57.5	16.0	25.0	0	1.5

Table 2. Slag composition of the solid solution with a matrix phase.

name	CaO	SiO_2	P_2O_5	FeO	Fe_2O_3
LL2+(1)	33.7	32.6	5.4	28.3	0
LL2+(2)	38.0	32.0	8.0	20.0	0
SL2+(1)	37.3	27.3	8.1	27.3	0
SL2+(2)	44.5	24.1	8.1	23.3	0
SL2+(3)	35.0	25.0	10.0	30.0	0
SL3+(1)	44.0	21.0	6.0	0	29.0
SL3+(2)	49.2	25.7	12.0	0	13.1

Table 3. Slag composition of synthesized steelmaking slag.

name	Heat Treatment
LL2+(1)	1673K×10min → 1573K×10min → W.Q.
LL2+(2)	
SL2+(1)	
SL2+(2)	
SL2+(3)	
SL3+(1)	1923K×1h → 1773K×15min → W.Q.
SL3+(2)	1923K×1h → 1723K×30min → W.Q.

Table 4. Heating pattern to make synthesized steelmaking slag.

2.2 Dissolution Experiment

The prepared oxide sample was ground into particles smaller than 53 μm (270 mesh).

One gram of the sample was put into 400 mL of ion-exchanged water. A Teflon container with a 500 mL capac-

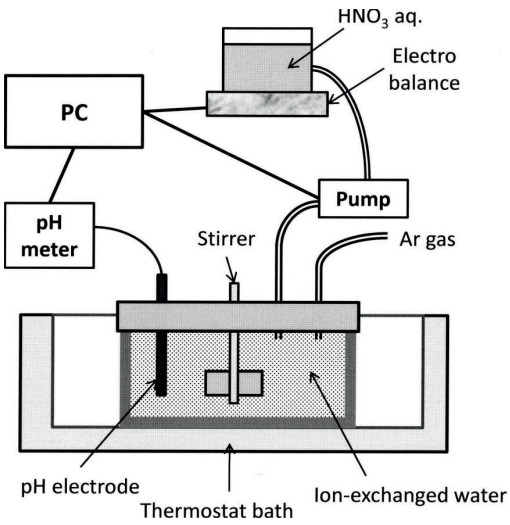

Figure 2. Schematic diagram of the experimental setup.

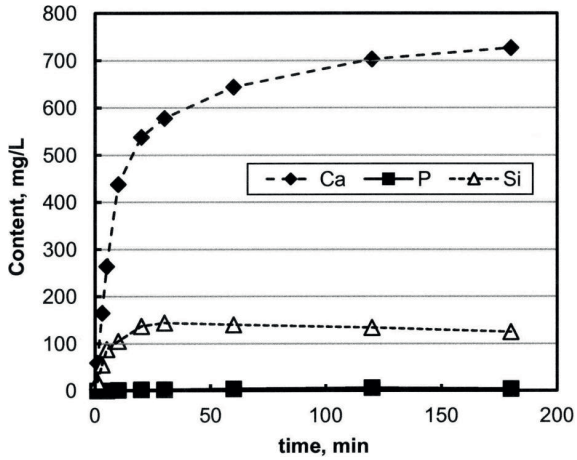

Figure 3. Change in element content in an aqueous solution over time (Sample 2).

ity was used as a vessel, and the temperature was kept constant at 298 K using an isothermal water bath. For deoxidizing the water, Ar gas was injected into the water at a flow rate of about 500 NmL/min, and the water was then agitated using a semicircular-shaped rotating stirrer of 60 mm in width at 140 rpm. To keep the pH at constant value, a pH meter was immersed and an aqueous solution of HNO_3 was automatically supplied using a PC control system. A schematic diagram of the experimental setup is shown in Figure 2. About 6 mL of water was sampled at adequate intervals and filtrated using a syringe filter (< 0.45 μm). Filtered water was analyzed using induction coupled plasma spectroscopy (ICP), and the residue on the filter was analyzed through X-ray diffraction.

3 Results

3.1 Dissolution Behavior of the Solid Solution

Typical behaviors of the change in concentration of Ca, Si, and P in water are shown in Figures 3 and 4 for samples 2 ($C_2S : C_3P = 9 : 1$) and 4 ($C_2S : C_3P = 7 : 3$), respectively, which were immersed in an aqueous solution of pH $= 7$. About 10 min after the start of the experiment, the pH could be maintained at a constant level, although it was difficult to control during the initial experiment period owing to a rapid increase. The dissolution ratio defined by equation (1) was calculated for each element and is shown in Figures 5 and 6.

$$\text{Dissolution ratio of M} = \frac{\text{Amount of M in aqua solution}}{\text{Amount of M in initial sample}} \quad (1)$$

For sample 4, the dissolution ratio of P increased for 30 min, and after reaching the maximum value, started to decrease. In contrast, the dissolution ratio of Ca and Si increased without reaching the maximum value. For sample 2, the dissolution ratio of Si reached the maximum value at 30 min, although the dissolution ratio of Ca increased without reaching the maximum value. In Table 1, the compound observed in the residue using X-ray diffraction analysis is summarized for each experiment. When the ratio of C_3P in the solid solution was lower than 0.2, amorphous SiO_2 was found, and when the ratio was higher than 0.3, the formation of hydroxyapatite (HAP; $Ca_5HO_{13}P_3$) was observed except in the cases of 0.6, 0.7 and pure C_3P. In these cases, the phases that were observed in the samples before the dissolution were found in the residues.

In this paper, the dissolution ratio after 180 min is generally defined as the "maximum dissolution ratio." However, when the P or Si content shows the maximum value during the dissolution test, the content of each element at this time is defined as the "maximum dissolution ratio"

The changes in the maximum dissolution ratio of Ca, P, and Si with the composition of the solid solution in an aqueous solution of pH $= 7$ are shown in Figure 7. The dissolution ratio of Ca was close to 1.0 in the case of pure C_2S and decreased greatly with an increase in the of C_3P content, while the dissolution ratio of P was about 0.1 and did not change by the C_3P content.

The changes in the maximum dissolution ratio of each element with pH for sample 4 are shown in Figure 8. For all elements, the dissolution ratios decreased with an increase in pH.

3.2 Dissolution Behavior of the Solid Solution with a Matrix Phase

The microstructure and composition of each phase for samples SS2+ and SS3+(1) are shown in Figure 9. In each case, the liquid fraction was very small, and most of the area was in a solid solution phase. The estimated ratio of

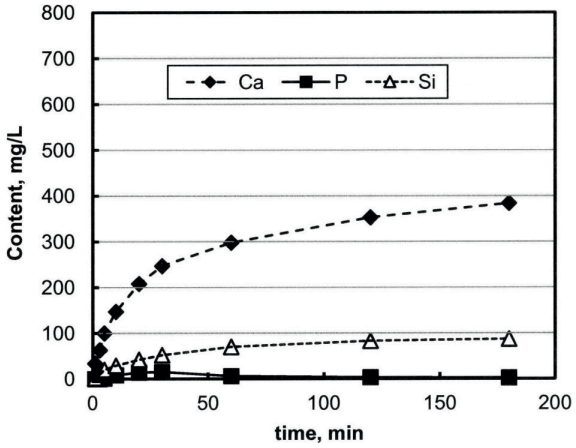

Figure 4. Change in element content in an aqueous solution over time (Sample 4).

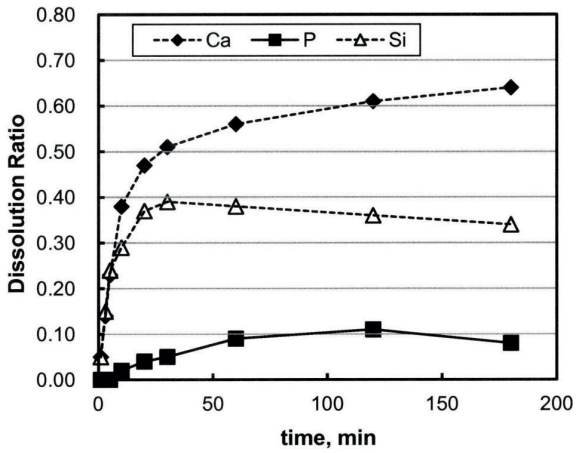

Figure 5. Change in the dissolution ratio of various elements over time (Sample 2).

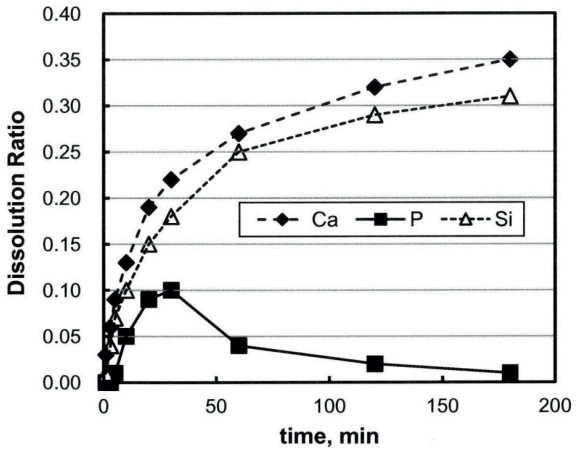

Figure 6. Change in the dissolution ratio of various elements over time (Sample 4).

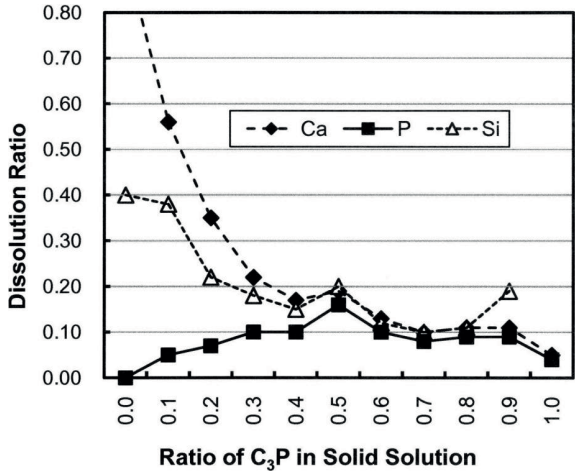

Figure 7. Changes in the maximum dissolution ratio of various elements with the composition of the solid solution.

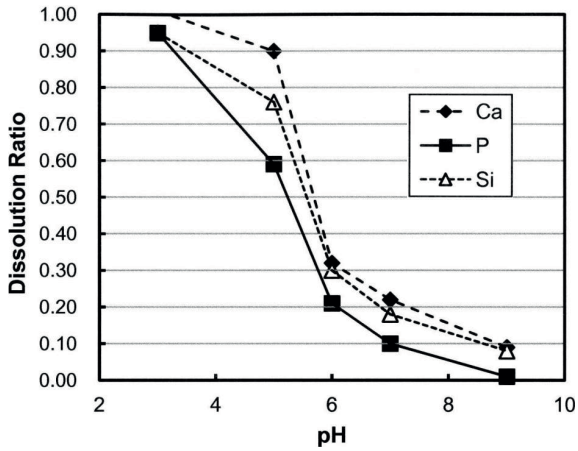

Figure 8. Change in the dissolution ratio of various elements with pH (sample 4).

C_2S : C_3P through an EPMA analysis was 6 : 4 for sample SS2+, 7 : 3 for SS3+(1), and 4 : 6 for SS3+(2). The FeO content in the solid solution was greater than 6%, while that of Fe_2O_3 was less than 1.5%.

The changes in maximum dissolution ratio of each element at pH = 7 are shown in Figure 10. When FeO was used as an iron oxide, the dissolution ratio was much lower than when Fe_2O_3 was used. Fe was not detected in the aqueous solution. The dissolution ratio of each element in samples SS3+(1) and SS3+(2) had a similar value as that of the solid solution shown in Figure 7.

3.3 Dissolution Behavior of Synthesized Steelmaking Slag

A solid solution phase was not observed in samples LL2+(1) and LL2+(2). These samples are considered to be in liquid form at the heating temperature, and a glassy structure was confirmed through X-ray diffraction analysis. A solid solution and a matrix phase were observed in the

Analyzed Point	Estimated Phase	Concentration (mass%)			
		CaO	SiO_2	P_2O_5	FeO
SS2+-1	Solid Solution	52.7	22.1	18.1	6.5
SS2+-2	Matrix	37.8	35.4	6.6	18.6

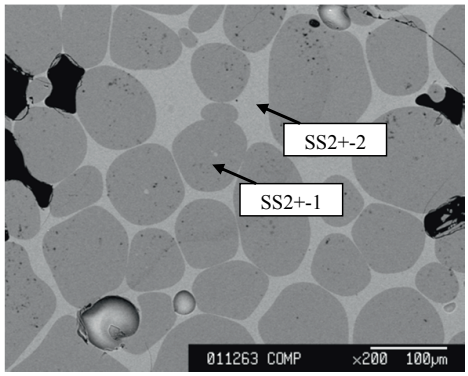

Analyzed Point	Estimated Phase	Concentration (mass%)			
		CaO	SiO_2	P_2O_5	Fe_2O_3
SS3+(1)-1	Solid Solution	58.9	24.1	15.5	1.3
SS3+(1)-2	Matrix	35.5	30.4	1.2	28.8

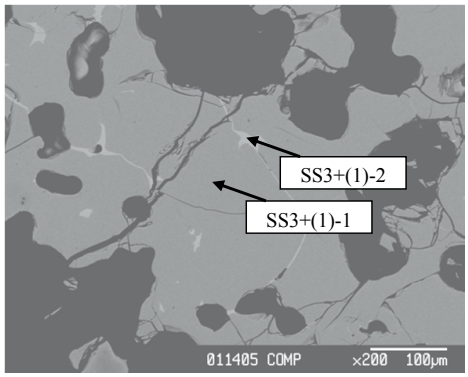

Figure 9. Microstructure and composition of each phase of the solid solution with a matrix phase.

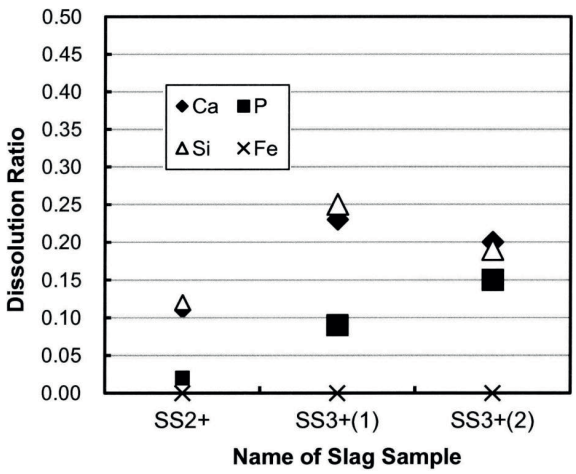

Figure 10. Dissolution ratio of various elements from the solid solution with a matrix phase.

other samples. The microstructure and composition of samples SL2+(2) and SL3+(1) are shown in Figure 11. The estimated ratio of $C_2S : C_3P$ was 6 : 4 for sample SL2+(1), 7 : 3 for SL2+(2), 4 : 6 for SL2+(3), 7 : 3 for SL3+(1), and 6 : 4 or 5 : 5 for SL3+(2). The FeO content in the solid solution was higher than 6 mass%, while that of Fe_2O_3 was lower than 2 mass% in almost all cases.

For the samples in which the solid solution and matrix phase were observed, the changes in the maximum dissolution ratio of each element at pH = 7 are shown in Figure 12. These results are very similar to the results shown in Figure 10: when FeO was used as the iron oxide, the dissolution ratio is much lower than when Fe_2O_3 was used. In all cases, Fe was not detected in the aqueous solution. In addition, the dissolution ratio of each element in samples SL3+(1) and SL3+(2) was similar to that in the solid solution. This indicates the possibility of extracting P from steelmaking slag even though the dissolution ratio is not sufficiently high.

Changes in the maximum dissolution ratio of each element with pH for the glassy sample are shown in Figure 13. For a comparison, the dissolving behavior of the solid solution (sample 4) shown in Figure 8 is given in this figure. The dissolution ratio of each element from the glassy sample was lower than that from the solid solution under every pH level. When the pH was higher than 7, dissolution from the glassy sample did not occur. Therefore, to extract P from slag, dissolution using water at pH = 7 can be considered appropriate.

4 Discussion

4.1 Dissolution Behavior of the Solid Solution

Although a stable compound in water is influenced by the Ca^{2+} content and pH level, $H_2SiO_3^0$ and $2HPO_4^{2-}$ can be considered the most stable products under this experimental condition [8]. The dissolving reactions and equilibrium constants of C_2S and C_3P at 298 K are expressed in equations (2) and (3). The equilibrium constants and activity coefficients were calculated using the same method reported by Miki et al. [6, 8].

$$2CaOSiO_2 + 4H^+ = 2Ca^{2+} + H_2SiO_3^0 + H_2O, \log K_1 = 27.561 \quad (2)$$

$$3CaOP_2O_5 + 2H^+ = 3Ca^{2+} + 2HPO_4^{2-}, \log K_2 = -6.56 \quad (3)$$

The solubility of Ca^{2+} calculated through these equations under the saturation of $H_2SiO_3^0$ or $2HPO_4^{2-}$ is shown in Figure 14 as a function of pH. Although in each case, the solubility increases with a decrease in pH, C_2S is much easier to dissolve compared with C_3P. This trend agrees qualitatively with the results shown in Figures 7 and 8.

Analyzed Point	Estimated Phase	Concentration (mass%)			
		CaO	SiO_2	P_2O_5	FeO
SL2+(2)-1	R	52.5	24.9	13.7	8.8
SL2+(2)-2	Matrix	29.9	31.1	0.7	32.4

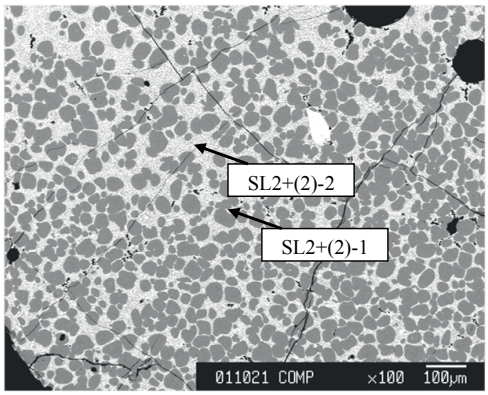

Analyzed Point	Estimated Phase	Concentration (mass%)			
		CaO	SiO_2	P_2O_5	Fe_2O_3
SL3+(1)-1	R	58.8	23.7	14.0	1.2
SL3+(1)-2	Matrix	28.0	15.4	0.5	55.7

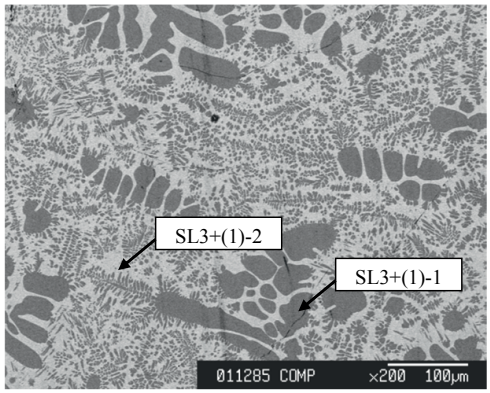

Figure 11. Microstructure and composition of each phase of synthesized steelmaking slag.

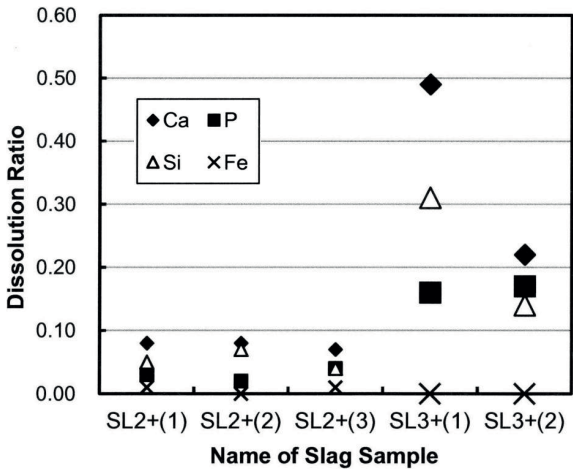

Figure 12. Dissolution ratio of various elements from synthesized steelmaking slag.

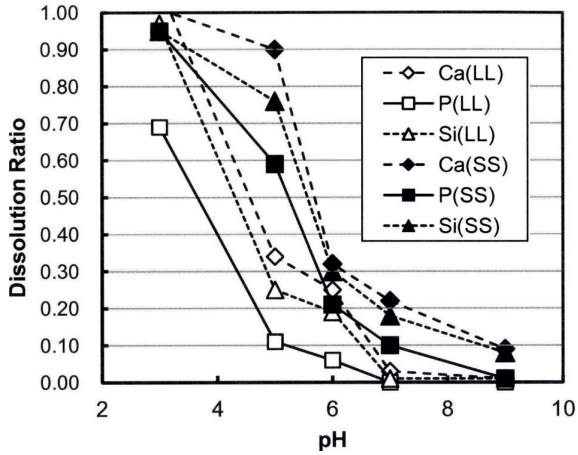

Figure 13. Difference in the dissolution behavior of various elements from glassy matrix (LL) and solid solution (SS) phases.

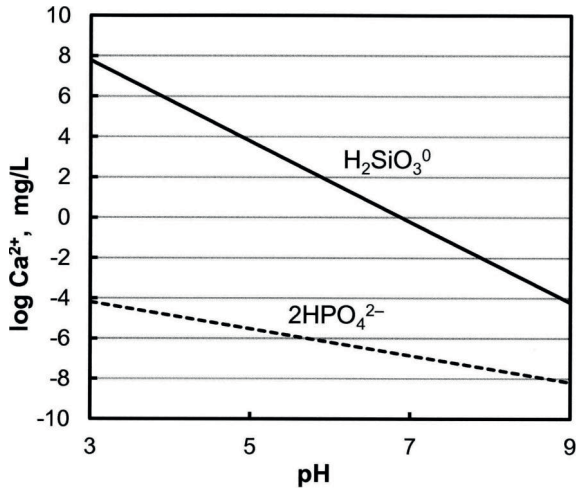

Figure 14. Solubility of pure $H_2SiO_3^0$ and pure $2HPO_4^{2-}$ in an aqueous solution at various pH levels.

The dissolving behavior of the solid solution is closely related to the solubility of the precipitate.

First, through stoichiometry, the expected contents of Si and P in water are calculated (Si_{cal}, P_{cal}) based on the Ca content in the aqueous solution and the concentration ratio of Si or P to Ca in the solid solution sample.

$$Si_{cal} = \text{Ca content in aqueous solution} \times (\text{Si content in sample/Ca content in sample}) \quad (4)$$

$$P_{cal} = \text{Ca content in aqueous solution} \times (\text{P content in sample/Ca content in sample}) \quad (5)$$

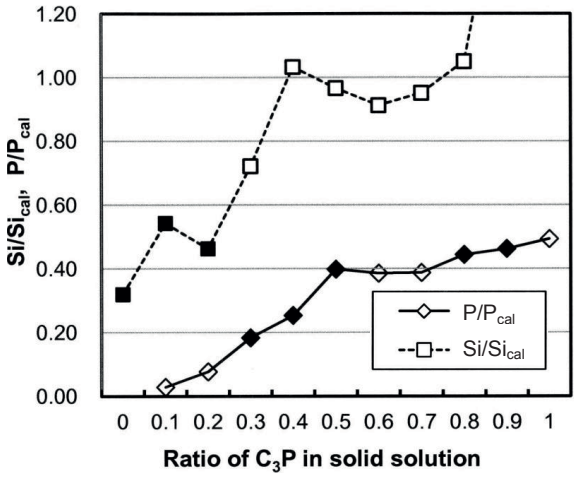

Figure 15. Ratio of the actual content in an aqueous solution to the expected contents through stoichiometry (experimental conditions under which amorphous SiO_2 or HAP were detected in the residues are shown in black marks).

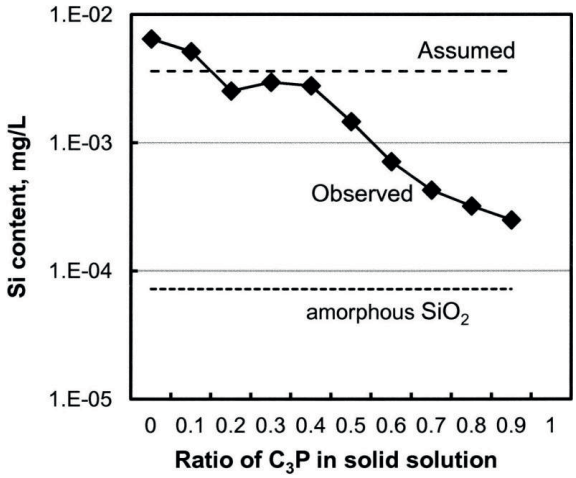

Figure 16. Comparison of the observed maximum Si content in an aqueous solution with the Si content calculated from equation (6) and assuming supersaturation.

The ratios of the actual content in an aqueous solution at the maximum dissolution ratio to the values calculated by equations (4) and (5) are summarized in Figure 15. In this figure, the experimental conditions under which amorphous SiO_2 or HAP was detected in the residues are shown with the black marks. From these results, the precipitation behavior in an aqueous solution can be considered as follows. When the ratio of C_3P is higher than 0.3, as the Si content is very close to Si_{cal}, precipitation of the Si-based compound does not occur. Therefore, when the P content reaches the level at which HAP precipitates, it shows the maximum value. On the other hand, when the ratio of C_3P is lower than 0.3, amorphous SiO_2 and HAP can precipitate, as the contents of Si and P are lower than Si_{cal} and P_{cal} However, it can be considered that the Si content rises to a level at which it precipitates the amorphous SiO_2 before the P content rises to a level at which it precipitates HAP.

Second, the precipitation conditions are calculated based on thermodynamics. Although a stable compound of Si is $H_2SiO_3^0$ under these experimental conditions, the Si content calculated from equation (2) is about 10^5 (mol/L) based on the average Ca content measured in this study. As this value is much greater than the Si content in this study, the precipitation of $H_2SiO_3^0$ will never occur. On the other hand, the Si content calculated by Eq. (6) is about 10^{-4}(mol/L) and is independent of the pH level. In Figure 16, the maximum Si content is compared with this value (Si_{sat}), and it can be seen that the precipitation of amorphous SiO_2 is possible at every pH.

$$SiO_2 + H_2O = H_2SiO_3^0, K_3 = -4.088 \qquad (6)$$

Although the stable compound of P was HPO_4^{2-} under these experimental conditions, HAP was detected in the residues. It is known that anhydrous dibasic calcium phosphate, ($CaHPO_4$, DCPA) or dibasic calcium phosphate dihydrate ($CaHPO_4 2H_2O$, DCPD) precipitates as a semistable compound and changes to HAP [9] The relation between HPO_4^{2-} and DCPA and that between HPO_4^{2-} and DCPD are written in equations (7) [10] and (8) [11], respectively.

$$CaHPO_4 = Ca^{2+} + HPO_4^{2-}, \quad K_4 = -6.90 \qquad (7)$$

$$CaHPO_4 2H_2O = Ca^{2+} + HPO_4^{2-} + 2H_2O, \quad K_5 = -6.59 \qquad (8)$$

In Figure 17, the P contents in an aqueous solution are compared with the P contents saturated with $3CaO \cdot P_2O_5$, DCPA, and DCPD calculated by equations (3), (7), and (8), respectively. It can be seen that the precipitations of these compounds are possible at every pH level.

To explain the precipitation behavior using a thermodynamic calculation, the lines calculated by assuming the supersaturation required to precipitate the compounds are drawn in Figures 16 and 17. In Figures 16 and 17, a value 50 times larger than that calculated from equation (6) and a value 10 times larger than that from equation (8), respectively, are assumed to be the critical conditions required to precipitate amorphous SiO_2 and DCPD. Compared with these lines to the content of Si and P in an aqueous solution, it can be considered that when the ratio of C_3P is higher than 0.3, the precipitation of DCPD occurs without the precipitation of amorphous SiO_2; however, when the ratio of C_3P is lower than 0.3, the precipitation of amorphous SiO_2 occurs without the precipitation of DCPD. These results agree with the experimental results, although it is imperative to clarify the meaning of the supersaturation values assumed in these calculations.

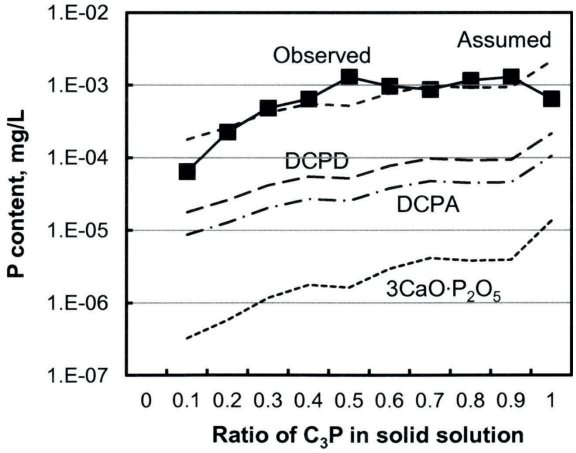

Figure 17. Comparison of the observed maximum P content in an aqueosu solution with the P content calculated from equations (3), (7), and (8) and assuming supersaturation.

4.2 Dissolution Behavior of the Solid Solution with a Matrix Phase and Synthesized Steelmaking Slag

As shown in Figures 10 and 12, when FeO was used as iron oxide, the dissolution ratio was much lower than when Fe_2O_3 was used. As the content of Fe in the aqueous solution was lower than the analytical limit under every condition, this difference is not be caused by the difference in the chemical reaction in the aqueous solution. On the other hand, it was previously observed [3] that the FeO content in the solid solution is higher than that of Fe_2O_3. The change in the composition of the solid solution is one of the reasons for this difference.

Through this study, the possibility to dissolve a solid solution containing P without dissolving the matrix phase was realized using an aqueous solution of pH $=$ 7. However, dissolving ratio of P was not high because of the precipitation of HAP, which formed with dissolved P and Ca. To overcome this disadvantage, the following two vessel process can be considered. First, before the contents of Ca and P reach the critical values of precipitation, the aqueous solution in the first vessel is transferred to the second vessel. Second, the pH of the transferred aqua solution is increased in the second vessel to precipitate the HAP and decrease the contents of Ca and P in the solution. This solution is then returned to the first vessel to redissolve the steelmaking slag. After this process is carried out repeatedly, it becomes possible to extract a solid solution from the matrix phase.

5 Conclusions

To clarify the possibility of the selective extraction of phosphorus from slag through a leaching process, the dissolution behavior of the solid solution of dicalcium silicate (C_2S) and tricalcium phosphate (C_3P) with various compositions and the matrix phase were investigated, and the following results were obtained.

(i) By measuring the dissolution behavior of the solid solution of C_2S-C_3P, it was found that the dissolution ratio of Ca was close to 1.0 in the case of pure C_2S and decreased greatly with an increase in the of C_3P content, while the dissolution ratio of P was about 0.1 and did not change by the C_3P content.

(ii) When the ratio of C_3P in the solid solution was lower than 0.2, amorphous SiO_2 was found in the residue, and when the ratio was higher than 0.3, the formation of HAP was observed except for the cases of 0.6, 0.7 and pure C_3P. The dissolution ratio of P increased for 30 min, and after reaching the maximum value, started to decrease owing to the precipitation of HAP.

(iii) By measuring the dissolution behavior of the solid solution with a matrix phase and the synthesized steelmaking slag, it was found that when FeO was used as iron oxide, the dissolution ratio was much lower than when Fe_2O_3 was used.

(iv) The dissolution ratio of each element from a glassy slag sample (matrix phase) was lower than that from the solid solution under every pH level. When the pH level was higher than 7, dissolution from the glassy sample did not occur.

From this study, the possibility to dissolve a solid solution containing P without dissolving the matrix phase was found through the use of an aqueous solution of pH $=$ 7. However, the dissolution ratio of P was not high because of the precipitation of HAP.

Acknowledgments

The authors appreciate the financial support of the Japan Society for the Promotion of Science (21360367), Grant-in-Aid for Scientific Research (B).

References

[1] S. J. Kim, T. Hotta, H. Shibata, S. Kitamura and K. Yamaguchi, "Fundamental Research to Produce Ferromanganese Alloy from Steelmaking Slag", *Proceedings of the 6^{th} European Slag Conference*, UNESID, Spain, Madrid, (2010), 183–192.

[2] T. Oda, I. Daigo, Y. Matsuno and Y. Adachi, "Substance Flow and Stock of Chromium Associated with Cyclic Use of Steel in Japan", *ISIJ International*, 50(2) (2010), 314–323.

[3] F. Pahlevani, S. Kitamura, H. Shibata and N. Maruoka, "Distribution of P_2O_5 between Solid Solution of $2CaO \cdot SiO_2$-$3CaO \cdot P_2O_5$ and Liquid Phase", *ISIJ International*, 50(6) (2010), 822–829.

[4] H. Ono, A. Inagaki, T. Masui, H. Narita, T. Mitsuo, S. Nosaka and S. Gohda, "Removal of Phosphorus from LD Converter Slag by Floating of Dicalcium Silicate during Solidification", *Tetsu-to-Hagane*, 66(9) (1980), 1317–1326.

[5] H. Kubo, K. Matsubae-Yokoyama and T. Nagasaka, "Magnetic Separation of Phosphorus Enriched Phase from Multiphase Dephosphorization Slag", *ISIJ International*, 50(1) (2010), 59–61.

[6] T. Futatsuka, K. Shitogiden, T. Miki, T. Nagasaka and M. Hino, "Dissolution Behavior of Nutrition Elements from Steelmaking Slag into Seawater", *ISIJ International*, 44(4) (2004), 753–761.

[7] W. Fix, H. Heymann and R. Heinke, "Subsolidus Relations in System $2CaO \cdot SiO_2$–$3CaO \cdot P_2O_5$", *J. Am. Ceram. Soc.*, 52(6) (1969), 346–347.

[8] T. Miki, K. Shitokiden, Y. Samada, T. Nagasaka and M. Hino, "Consideration of Dissolution Behavior of Elements in Steelmaking Slag Based on Their Stability Diagram in Seawater", *Tetsu-to-Hagane*, 89(4) (2003), 388–392.

[9] M. J. J. M. Kemenade and P. L. Bruyn, "A Kinetic Study of Precipitation from Supersaturated Calcium Phosphate Solutions", *J. Colloid Interface Sci.*, 118(2) (1987), 564–585.

[10] H. McDowell, W. E. Brown and J. R. Sutter, "Solubility Study of Calcium Hydrogen Phosphate. Ion-Pair Formation", *Inorganic Chemistry*, 10(8) (1971), 1638–1643.

[11] T. M. Gregory, E. C. Moreno and W. E. Brown, "Solubility of $CaHPO_4 \cdot 2H_2O$ in the System $Ca(OH)_2$-H_3PO_4-H_2O at 5, 15, 25 and 37.5°C", *J. Res. NBS* 74A(4) (1970), 461–475.